PADÉ APPROXIMANTS AND AN ELECTROMAGNETIC FORMFACTOR IN Φ^4 MODEL*

By M. Pindor

Institute of Theoretical Physics, University of Warsaw**

(Received November 15, 1977)

In the paper an analytic structure of the electromagnetic formfactor of pseudoscalar particles, interacting via Φ^4 hamiltonian, in the coupling constant complex plane is studied and a possibility of applying Padé Approximants (PA) to its perturbation series is considered. The study is based (in the elastic approximation) on the Omnès equation. Serious difficulties are anticipated when trying to apply PA to the series. This conclusion is supported by negative numerical results obtained up to fourth order. For illustration, a simplified model is considered wherein one can study analytic structure of the formfactor in more detail and also the perturbation expansion up to eighth order can be found without excessive difficulties.

1. General remarks

Padé Approximants (PA) [1] have shown to be a useful calculational tool in many problems of theoretical physics [2]. It has been proved in the framework of potential model that, for many physically interesting functions, PA formed from power expansions of these functions converge to exact values [3]. The situation is much less clear in models of quantum field theory. Here, as far as we know, only numerical investigations have been made, and moreover, because of difficulties in calculating higher order expansions, only lowest order terms have been found and PA constructed from them compared with experiment [2].

Such a procedure, while offering a satisfaction from "doing physics", sheds little light on both, applicability of PA to a particular model and an adequacy of the model for a given physical process.

There is, however, one notable exception. We mean the $\pi-\pi$ scattering described in Φ^4 model. Here, it turned out to be possible [4] to calculate S matrix up to the fourth order and compare results from third and fourth orders (to study scattering in $T = 1$, $l = 1$ channel in the third order one had to use K matrix approach because up to this order S

* The study was supported by the Polish Ministry of Higher Education, Science and Technology, project M.R.I. 7.

** Address: Instytut Fizyki Teoretycznej, Uniwersytet Warszawski, Hoża 69, 00-681 Warszawa, Poland.

matrix has no unitarity cut [5]). They were quite similar what suggested a convergence (the fast one!) of PA for the S matrix perturbation expansion in that model. A compatibility of those results with the experimental information on $\pi-\pi$ scattering, particularly in $T=1$, $l=1$ channel, was also of a great importance.

There exists, however, other experimentally measurable function describing $\pi-\pi$ interaction — namely the electromagnetic formfactor of pion. If one adds to the Φ^4 model lagrangian a standard minimal coupling with an electromagnetic field, then it is possible to find the formfactor up to fourth order in the $\pi-\pi$ coupling constant. Feynman diagrams contain one loop more than corresponding diagrams for the amplitude and therefore calculations are more difficult but resulting expressions are still numerically tractable.

The formfactor, particularly in the elastic approximation described below, is closely related to the amplitude, but its perturbation expansion is entirely different. Therefore, it seems interesting to see what happens with its PA. Even if, in analogy to the results obtained for the amplitude, one expects a fast convergence, there are still many questions which seem to be interesting and cannot be answered a priori. One can ask e.g. which PA will be the best ones for the formfactor — there is no guiding principle like unitarity, here, which could select the diagonal PA; what will be a width of ϱ obtained here? One could also study an influence of inelastic contributions on ϱ parameters. As will be shown below, these questions cannot be answered at all because analytic properties of the formfactor in the coupling constant plane seem to exclude a convergence of PA in the physical region of the coupling constant.

Although the present study may seem slightly obsolate and does not conform with the recent trend of exploiting a connection between variational principles and PA [6] we think it brings some new and nonobvious information.

2. *The electromagnetic formfactor in Φ^4 model*

We use the notation of Bjørken and Drell [7] and follow closely definitions of [4]. The formactor $F(q^2)$ is defined by

$$\langle \pi^+\pi^- \text{ out}|j_\mu(q)|0\rangle = -\frac{i(2\pi)^4\delta^4(q-p_+-p_-)}{(2\pi)^3\sqrt{4\omega_+\omega_-}}(p_+-p_-)^\mu F(q^2+i\varepsilon), \tag{2.1}$$

$$j_\mu(q) = \int d_4z e^{-iqz} j_\mu(z), \tag{2.2}$$

$$j_\mu(z) = i{:}[\varphi_-(z)\partial_\mu\varphi_+(z)-\varphi_+(z)\partial_\mu\varphi_-(z)]{:}. \tag{2.3}$$

Hamiltonian density for Φ^4 coupling of pions is

$$\mathscr{H}(x) = g_0/4{:}(\varphi_\alpha(x)\varphi^\alpha(x))^2{:}, \tag{2.4}$$

where g_0 is an unrenormalized coupling constant. The renormalized coupling constant is defined by

$$A^T(s=\tfrac{4}{3}, t=\tfrac{4}{3}, u=\tfrac{4}{3}) = g\begin{cases} 10 & T=0 \\ 0 & T=1. \\ 4 & T=2 \end{cases} \tag{2.5}$$

Normalization of A^T can be seen from

$$S_{fi} = \delta_{fi} - i \frac{(2\pi)^4}{(2\pi)^6 (2\omega)^2} \delta^4(P_i - P_f) \sum_{T=0}^{2} A^T(s, t, u) \boldsymbol{P}^T, \tag{2.6}$$

S_{fi} being $\pi - \pi$ scattering matrix and $\boldsymbol{P}^T$ isospin projection operator.

It is well known [7] that $F(q^2)$ satisfies the following dispersion relation

$$F(s) = F(0) + \frac{s}{\pi} \int_4^\infty \frac{\operatorname{Im} F(s')}{s'(s' - s - i\varepsilon)} ds'. \tag{2.7}$$

The pion mass will be taken henceforth as a unit. (2.7) should be understood modulo a number of necessary subtractions. It appeared, however, that one subtraction has been sufficient to make all integrals converging, up to the fourth order.

We concentrated our study of the formfactor on a search for the ϱ meson pole. This is well known to dominate the experimental shape of the formfactor for low values of q^2 [8], and it can be shown that the appearance of this pole on the unphysical sheet of F is a natural consequence of (2.7). Therefore we decided to use equation (2.7) and calculate consecutive orders of F in the iterative way, exploiting a condition expressing Im F through contributions from elastic intermediate states and neglecting inelastic ones. As it is well known ϱ couples weekly to four pion states, so such an approximation should not influence its parameters much and cannot endanger its existence.

We recall that the pole appeared in the amplitude without taking into account inelastic intermediate states. Thus we think it to be reasonable to start calculations with a simplified expression for ImF

$$\operatorname{Im} F(s) \underset{s>4}{=} -\frac{1}{32\pi} \sqrt{\frac{s-4}{s}} A^{T=1, l=1}(s - i\varepsilon) F(s + i\varepsilon) \tag{2.8}$$

and only after finding the pole on the unphysical sheet, eventually to try to improve its parameters by adding inelastic contributions to ImF.

After making this approximation we obtain an interesting information on a behaviour of F in the complex coupling constant plane using analogous information on $A^{T, l}$ as an input. One could argue that too little is known about the latter to draw any conclusions about the former. It happens, however, that it is sufficient to assume an existence of the ϱ pole and the way it behaves with changing value of the coupling constant, to find information on the analytic structure of F which is crucial for a behaviour of PA to F. It is assumed below that for growing values of the coupling constant g the ϱ pole approaches the threshold, to reach it at some value g_T, and becomes a bound state for $g > g_T$. The ϱ pole stays on the unphysical sheet for $g < g_T$ and escapes to infinity when $g \to 0$. Such a behaviour of a resonance pole seems to be perfectly reasonable and takes place for virtual states in potential models. Moreover, Bessis and Pusterla [4] found that when they changed g near the value corresponding to the physical ϱ mass, the pole moved in agreement with the above assumption.

3. Analytic properties in the complex coupling constant plane

Inserting (2.8) into (2.7) and using an obvious condition $F(0; g) \equiv 1$ we have

$$F(s; g) = 1 - \frac{s}{32\pi^2} \int_4^\infty \sqrt{\frac{s'-4}{s'}} \frac{A^{T=1,I=1}(s'-i\varepsilon; g) F(s'+i\varepsilon; g)}{s'(s'-s-i\varepsilon)} ds'. \tag{3.1}$$

This is the Omnès equation [9] when we neglect intermediate states also in the unitarity condition for $A^{T=1, I=1}$

$$\operatorname{Im} A^{T=1,I=1}(s; g) \underset{s>4}{=} -\frac{1}{32\pi} \sqrt{\frac{s-4}{s}} |A^{T=1,I=1}(s; g)|^2. \tag{3.2}$$

A particular solution of this equation is the Omnès function

$$F(s; g) = \exp\left[\frac{s}{2\pi i} \int_4^\infty \frac{ds'}{s'(s'-s-i\varepsilon)} \log \frac{A^{T=1,I=1}(s'+i\varepsilon; g)}{A^{T=1,I=1}(s'-i\varepsilon; g)}\right]. \tag{3.3}$$

Although it is not the only solution of (3.1) it can be shown to have expansion in powers of g identical with the series obtained by iteration of (3.1) — so it is the solution we are interested in.

Now we can study, by using standard methods, singularities of F, assuming the properties of $A^{T=1, I=1}$ as in the previous section.

The singularities are of two types: (a) pinching singularities, (b) end-point singularities.

(a) We consider only singularities arising from pinching of the contour between a zero of the denominator and the pole of $A^{T=1, I=1}$. As the pole of $A^{T=1, I=1}$ lies on the unphysical sheet and does not depend on s (but on s'), to obtain pinching with the s dependent denominator, we must push s from the upper half plane of the physical sheet to the lower half plane of the unphysical one. When s crosses the integration contour we must add

$$\frac{2\pi i}{s} \log \frac{A^{T=1,I=1}(s+i\varepsilon; g)}{A^{T=1,I=1}(s-i\varepsilon; g)}$$

o the integral and therefore F on the unphysical sheet is given by

$$F_{\text{unph}}(s; g) = \frac{A^{T=1,I=1}_{\text{unph}}(s; g)}{A^{T=1,I=1}(s; g)} F(s; g). \tag{3.4}$$

A and F without the subscript mean values on the physical sheet (lower half plane).

We immediately see that $F_{\text{unph}}(s; g)$ has a pole for the value of s for which $A^{T=1, I=1}_{\text{unph}}$ — an analytic continuation of $A^{T=1, I=1}(s+i\varepsilon; g)$ to the lower half plane — has also one. It is just how unphysical sheet poles of $A^{T=1, I=1}$ induce unphysical sheet poles of F.

A position of this pole in the g-plane depends on s.

(b) Singularities coming from approaching end-points of the integration path by singularities of $A^{T=1,\,l=1}$ are s independent and they can appear only at $g = g_T$ and $g = g_0$. Moreover one can expect that F has cuts for such values of g (complex) for which the pole of $A^{T=1,\,l=1}$ lies on the integration path.

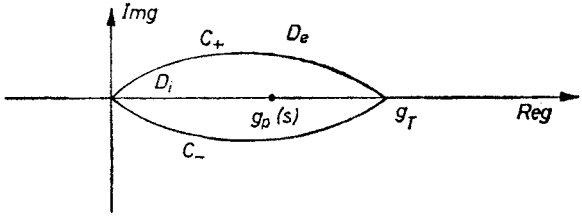

Fig. 1. Singularities of $F(s; g)$ in the complex g plane

To see whether for these values of g we really have a discontinuity of F we must calculate a change of F when the pole of $A^{T=1,\,l=1}$ crosses the integration contour of (3.3).

Let $C_{\pm}$ be a set of values of g for which an analytic continuation of $A^{T=1,\,l=1}(s+i\varepsilon; g)$ has a pole for $s > 4$. $C_+^* = C_-$ because

$$(A^{T=1,l=1}(s; g))^* = A^{T=1,l=1}(s^*; g^*). \tag{3.5}$$

Now let us consider what happens in s' plane ($g_p(s)$ denotes a value of g for which the ϱ pole appears at a position s on the unphysical sheet of $A^{T=1,\,l=1}$).

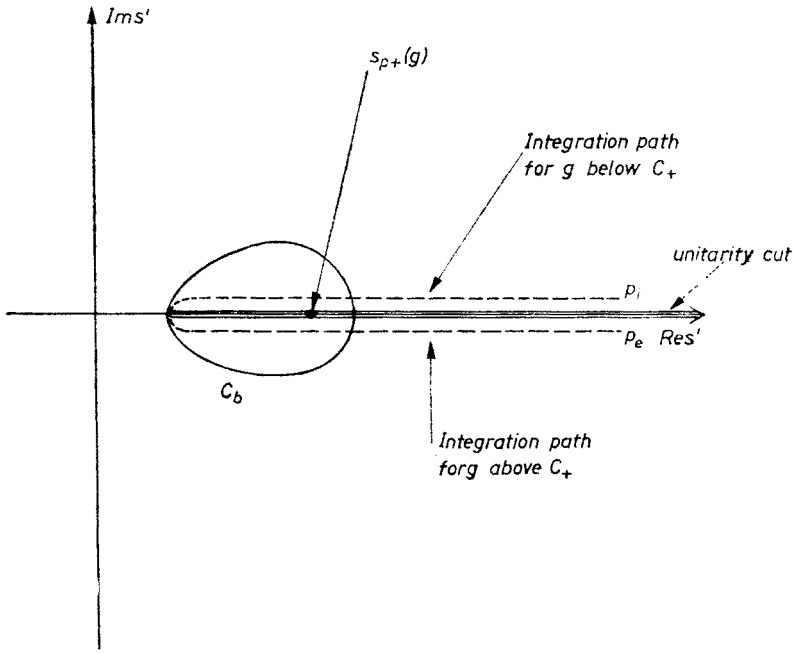

Fig. 2. Contour of integration in the calculation of A_+ in (3.6)

Drawing Figs 1 and 2 we have assumed that the ϱ pole approaches the real axis from below when Img grows but the inverse could also be assumed and it would result only in the interchange of C_+ and C_-. Thus when g approaches C_+ from below, the pole approaches half-axis $s > 4$ also from below. It is depicted on Fig. 2 by shifting the integration path p_i slightly above the real axis. When g is above C_+, the pole is above the real axis. This is again shown on Fig. 2 by shifting the integration path p_e below the real axis.

Subscripts "e" and "i" mean exterior and interior of the loop formed by C_+ and C_- and the corresponding parts of the complex plane are D_e and D_i.

An analytic continuation of $A^{T=1,\, l=1}(s' \pm i\varepsilon; g)$ in the neighbourhood of the half-axis $s' > 4$ will be henceforth denoted $A_\pm$ and $s_{p\pm}(g)$ will be a position of the pole of $A_\pm$ as a function of g.

Now we are interested in a difference

$$\Delta_+ = \int \frac{ds'}{s'(s'-s)} \log \frac{A_+(s'; g)}{A_-(s'; g)}\bigg|_{g\in D_e} - \int_{p_i} \frac{ds'}{s'(s'-s)} \log \frac{A_+(s'; g)}{A_-(s'; g)}\bigg|_{g\in D_i} . \tag{3.6}$$

It can easily be seen to be equal to

$$\int_{C_b} \frac{ds'}{s'(s'-s)} \log \frac{A_+(s'; g)}{A_-(s'; g)},$$

C_b is as shown on Fig. 2. Taking into account the obvious assumption that the ϱ pole is a single pole we see that $A_\pm(s'; g) \cdot (s' - s_{p+}(g))$ is regular inside C_b and therefore

$$\Delta_+ = \int_{C_b} \frac{ds'}{s'(s'-s)} \log \frac{A_+(s'; g) \cdot (s'-s_{p+})}{A_-(s'; g)} - \int_{C_b} \frac{ds'}{s'(s'-s)} \log (s'-s_{p+})$$

$$= -\int_{C_b} \frac{ds'}{s'(s'-s)} \log (s'-s_{p+}) = 2\pi i \int_4^{s_{p+}} \frac{ds'}{s'(s'-s)} = \frac{2\pi i}{s} \log \left[\frac{s_{p+}(g)-s}{s_{p+}(g)} \cdot \frac{4}{4-s}\right],$$

and then

$$F_{e+}(s; g) = F_i(s; g) \cdot \frac{s_{p+}(g)-s}{s_{p+}(g)} \cdot \frac{4}{4-s} . \tag{3.7}$$

F_{e+} means a continuation of F from D_e through C_+.

Analogously

$$F_{e-}(s; g) = F_i(s; g) \cdot \frac{s_{p+}(g)-s}{s_{p+}(g)} \cdot \frac{4}{4-s} . \tag{3.8}$$

We recall that $s_{p-}(g)$ is a position of a pole of A_- on the upper half plane of the unphysical sheet (i.e. the upper half plane obtained by a continuation of $A(s'-i\varepsilon; g)$ from the lower

half-plane of the physical sheet through the unitarity cut). It is visible now that zero and g_T are really branch points of F_e. Moreover F_i and F_e are different analytical functions and cannot be obtained one from the other by an analytic continuation along any path.

One can easily see that just F_i is a physical formfactor, because it is this function which is a solution of (3.1) for $g > 0$.

An interesting observation can be made that g_T is not a branch point of F_i. Indeed, if we denote by F_{i+} and F_{i-} analytic continuations of F_i through C_+ and C_- respectively, then

$$F_{i+}(s; g) = F_e(s; g) \cdot \frac{s_{p+}(g)}{s_{p+}(g) - s} \cdot \frac{4-s}{4} \tag{3.9}$$

and

$$F_{i-}(s; g) = F_e(s; g) \cdot \frac{s_{p-}(g)}{s_{p-}(g) - s} \cdot \frac{4-s}{4}. \tag{3.10}$$

If now $g > g_T$ then $0 < s_{p\pm}(g) < 4$, but as

$$s^*_{p+}(g) = s_{p-}(g) \tag{3.11}$$

(because of (3.5)) then for $g > g_T$, $s_{p+}(g) = s_{p-}(g)$ and

$$F_{i+}(s; g) \underset{g > g_T}{\equiv} F_{i-}(s; g). \tag{3.12}$$

However, $g = 0$ is a branch point of F_i because $A_\pm$ cannot have poles on real s axis for $g < 0$.

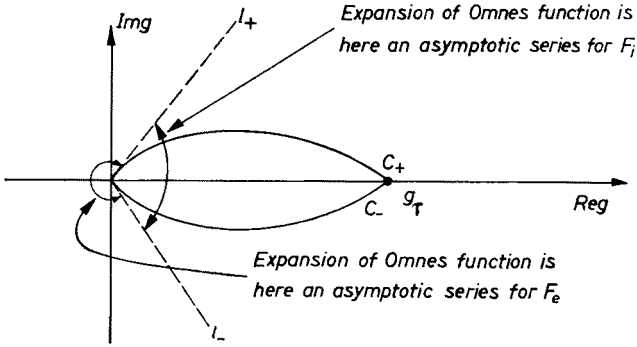

Fig. 3. Conjectured sectors of convergence of PA for F

Straight lines tangent to C_+ and C_- at $g = 0$ (l_+ and l_- on Fig. 3) divide the complex plane into two sectors. Series obtained from a power expansion of the r.h.s. of (3.3) is an asymptotic expansion of F_e in the left sector and of F_i in the right one (Fig. 3).

If we make now a wishful assumption that PA converge somewhere near the origin, the question is: what is a function they converge to? We do not have any theorem that

could be applied in our situation, and we can, therefore, only make more or less plausible speculations. We expect that PA would converge to F_e in the left sector and to F_i in the right one. If this were true, a rate of convergence on the positive semi axis would depend crucially on the angle between l_+ and l_- and in a case it was small, the convergence would be very slow and would change into divergence if it were zero.

Thus we conjecture that even in a case of a perfect convergence of PA constructed from the perturbation series for the scattering amplitude, there can be serious defficulties with convergence of PA for the formfactor just in the region of physical values of the coupling constant. Whether or not these difficulties actually arise depends however on details of the model and can only be checked numerically.

We want to stress that the above conclusions should also be valid when inelastic channels are included. Indeed, if they were to cancel singularities introduced by elastic channels, we would not observe the ϱ pole in the formfactor experimentally.

4. Calculation of PA up to the fourth order

Keeping in mind what we have learned from the above considerations we can calculate perturbation expansion terms for the formfactor up to the fourth order and see what happens with corresponding PA. Because of $F(0; g) \underset{g}{\equiv} 1$ and $A_1^{T=1,\, l=1}(s) \underset{s}{\equiv} 0$, the series takes the form

$$F(s; g) = 1 + g^2 F_2(s) + g^3 F_3(s) + g^4 F_4(s). \tag{4.1}$$

We used terms of the perturbation expansion for $A^{T=1,\, l=1}$ calculated in [4][1] and inserted them into (2.8) and then we calculated dispersion integral (2.7). In second and third orders we were able to perform almost all integrals analytically and the corresponding formulae are presented in Appendix A.

There were, however, nontrivial numerical difficulties in the fourth order. According to [4] $A_4^{T=1,\, l=1}$ can be expressed as follows

$$A_4^{T=1,\, l=1}(s) = A_{AB}(s) + A_\varphi(s) + A_R(s) + A_{\tilde{R}}(s) + A_f(s), \tag{4.3}$$

---

[1] Checking formulae in [4] we were unable to make our expressions for $P(s)$ compatible with C.19 in [4]. In our opinion

$$P(s) = \frac{1}{s} \int_0^{\frac{1}{2}\sqrt{s-16}} x\,dx \int_{\sqrt{4+x^2}}^{\sqrt{s}-\sqrt{4+x^2}} \frac{dy}{\sqrt{s}-y}$$

$$\sqrt{\frac{y^2-x^2-2y\sqrt{s}+s-4}{y^2-x^2-2y\sqrt{s}+s}}\ \log \frac{\sqrt{y^2-x^2}\,(\sqrt{s}-y)+x\sqrt{y^2-x^2-4}}{\sqrt{y^2-x^2}\,(\sqrt{s}-y)-x\sqrt{y^2-x^2-4}}. \tag{4.2}$$

There was also an obvious misprint in C.16.

where

$$A_i(s) = \frac{4}{\pi(s-4)} \int_4^\infty f_i(s, t') Q_1\left(1 + \frac{2t'}{s-4}\right) dt', \tag{4.4}$$

$$f_i(s, s') = \begin{cases} -\dfrac{1}{32\pi}\sqrt{\dfrac{s'-4}{s'}}\left\{\frac{1}{3}[A_0(s')+B_0(s')] - \frac{5}{6}[A_2(s')+B_2(s')]\right\}, & i = AB, \\ \dfrac{20}{(2\pi)^6}\dfrac{1}{\sqrt{s'(s'-4)^3}} \displaystyle\int_4^\infty dt' \int_4^\infty dt'' \sqrt{\dfrac{(t'-4)(t''-4)}{t't''}} \\ \quad \times [4\varphi(\xi, \eta, z) - \varphi(\xi, \eta, -z) - 3Q_0(\xi)Q_0(\eta)], & i = \varphi, \\ -25R(s', s), & i = R, \\ -5R(s', 4-s-s'), & i = \tilde{R}, \\ f(s'), & i = f. \end{cases} \tag{4.5}$$

Definitions of $A_{0,2}$, $B_{0,2}$, φ, R and f are the same as in [4].

All A_i except for $i = AB$ are expressed as triple integrals, so that finally F_4 is expressed by quadruple integrals. To calculate them we used iteratively subroutines INTGSX (described in [10]) and CPINTX — its version for complex-valued functions.

A difficulty arises from the fact that A_φ has an imaginary part coming from inelastic contributions in direct channel and it makes $\mathrm{Im}F_4$ complex. Of course, the full $\mathrm{Im}F_4$ is real but it results from cancellation of the imaginary part of A_φ with contributions of intermediate inelastic states directly to $\mathrm{Im}F_4$, and we have neglected the latter. Therefore, for compatibility, we should neglect inelastic contributions to A_φ. It is impossible in this form, as we have to continue A_φ analytically to the unphysical sheet (to have the formfactor there) and its imaginary part contains $\vartheta(s-16)$. A_φ contains also contributions from elastic intermediate states in the crossed channel, and therefore it cannot be neglected as a whole.

It is naturally possible to express A_φ in a different form with contributions from intermediate states in direct channel decoupled from crossed channel elastic contributions but such expressions would contain one integration more and it was outside our numerical possibilities to calculate them.

We have decided therefore to leave A_φ in the form given above. In this way we had real-hermiticity of F on the physical sheet broken, but we thought that a size of the breaking is a good measure of an error we made leaving A_φ complex. We checked a large area of the physical sheet and found that $|F_4(s^*) - F_4^*(s)|$ was never larger than 0.5%. Later, however, an unwanted phenomenon occurred for which, we thought, was just $\mathrm{Im}A_4(s > 16)$ responsible. We comment on this below.

Having calculated F_2, F_3 and F_4 we were able to construct:
[0/2] from the second order,
[0/3], [1/2], [2/1] from the third order,
[0/4], [1/3], 2/2], [3/1] from the fourth order.
Their explicit forms are given in Appendix B.

To study their singularities in the complex g-plane we used the following tactics. We calculated $[M/N]_F$ for a given s and we found values of g making denominators of PA to vanish. Then, changing s, we looked for points (of the complex s plane) at which imaginary parts of those g were zero. Lines in the s-plane found this way will be called henceforth

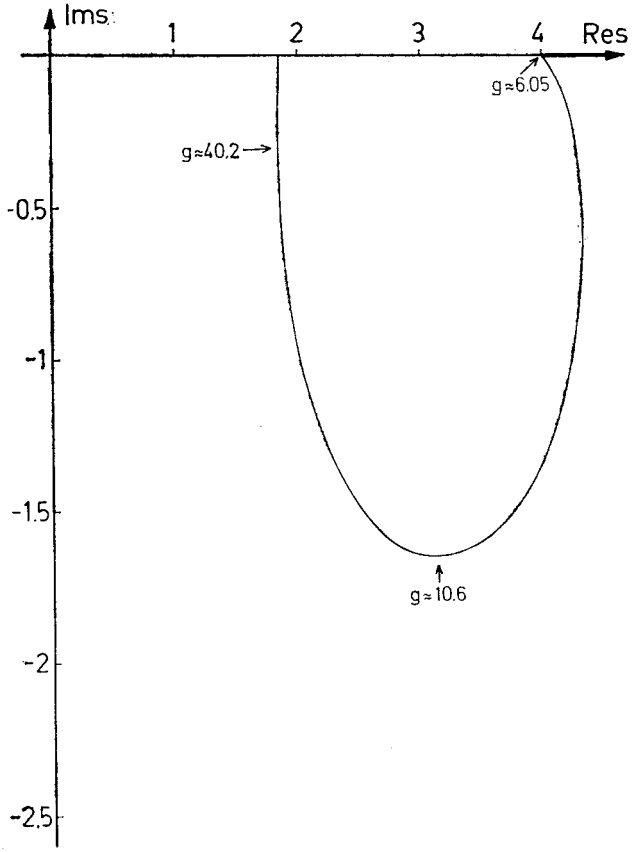

Fig. 4. An orbit of one of the poles of $[1/2]_F$

orbits of poles. We concentrated our attention on the orbits passing through the threshold. All others had large Img in a considerable area of the s plane near the threshold and we thought therefore that they could not be suspected of reproducing resonance poles. Unfortunately, even orbits passing through the threshold did not seem to have much in common with the expected ϱ orbit. They generally form small loops near the threshold and moreover exhibit a wrong dependence on Reg. Poles situated on them move toward

the threshold when Reg diminishes in contrast to what we expect (see Section 2). Therefore we think they have nothing to do with true poles of F. An example of such an orbit is given on Fig. 4.

In each order there was a pole of $[0/N]_F$ which behaved differently. Orbits of those poles with values of Reg marked on them are shown on Fig. 5. One can see that the orbit of a pole of $[0/4]F$ passes through the physical sheet near the threshold. We attribute this just to a lack of real-hermiticity of F. Such a view is supported by the proper behaviour

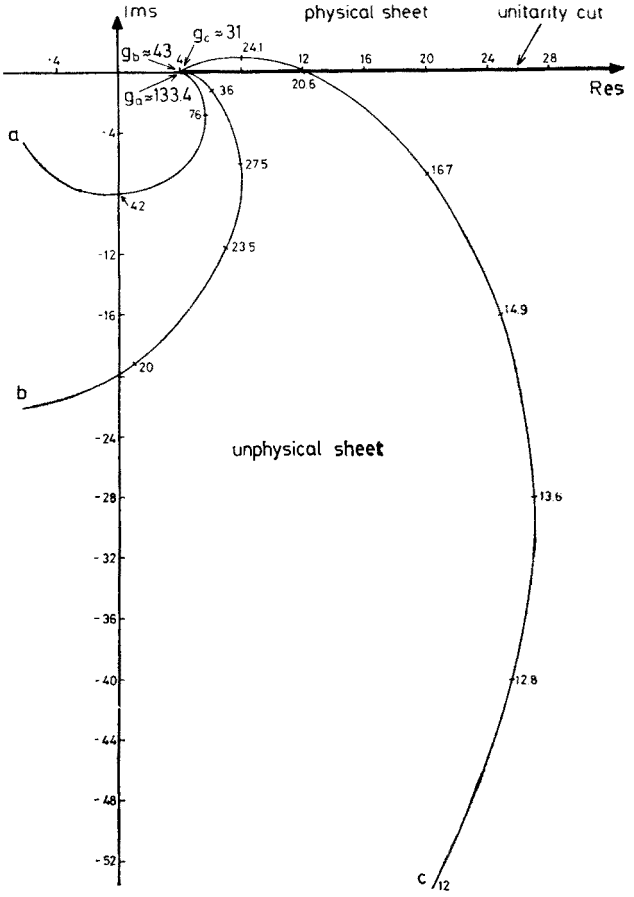

Fig. 5. Orbits of poles of $[0/N]_F$

of the analogous orbit in the simplified model considered in Section 5. There, $F_n(s)$ is real-hermitian for all n. Also none of these orbits resembles an expected ϱ orbit (which should pass through $s \approx 30 - 10i$ for $g \approx 6$) though they seem to change their shapes in the good direction, as order of the perturbation theory increases.

Concluding we can say that the ϱ pole does not appear in low order PA for the form-factor in contrast to what happens for the scattering amplitude. It is in full agreement

with considerations of Section 3 suggesting that an angle between curves C_+ and C_- (Fig. 3) is small. The behaviour of orbits on Fig. 5 suggests that the latter is not zero, and therefore that it could be possible to obtain an agreement with results found for the amplitude if higher orders were calculated.

5. *A simplified model*

We can illustrate considerations of the last two Sections discussing a simplified model, which has however many realistic features. The general idea behind this simplification is to take an approximate amplitude, which would have however proper analytic structure, and a ϱ-like orbit on the unphysical sheet and insert it into the Omnés equation. If one were clever enough in approximating the amplitude, so that many orders of its power expansion could be calculated without undue hardship, then one could see what happens with higher order PA. All these requirements are satisfied if one takes for the amplitude (the form of it has been suggested to the author by J. L. Basdevant)

$$A^{T=1,I=1}(s;g) \approx A = \frac{1}{\varrho}\frac{[2/1]_{K^{11}}}{1-i[2/1]_{K^{11}}}, \tag{5.1}$$

where

$$\varrho = -\frac{1}{32\pi}\sqrt{\frac{s-4}{s}}$$

and $[2/1]_{K^{11}}$ is the corresponding PA for $K^{T=1,I=1}(s;g)$. Because of the lack of the unitarity cut in $A_2^{T=1,I=1}$ and $A_3^{T=1,I=1}$ we could not take $[2/1]_{A^{11}}$ for the same purpose as above.

It is easy to check that

$$K_{2,3}^{T=1,I=1} = \varrho A_{2,3}^{T=1,I=1} \quad \text{and} \quad [2/1]_{K^{11}} = \frac{g^2 K_2^{11}}{1-g\dfrac{K_3^{11}}{K_2^{11}}}, \tag{5.2}$$

thus finally

$$A(s;g) = \frac{g^2 A_2(s)}{1-A_3(s)/A_2(s)\cdot g + \dfrac{i}{32\pi}\sqrt{\dfrac{s-4}{s}}\,A_2(s)\cdot g^2} \tag{5.3}$$

(we use A_i for $A_i^{T=1,I=1}$).

A numerical study of this function shows that it has a pole on the unphysical sheet for $g < g_T \approx 14.54$. For higher values of g the pole lies below the threshold and imitates the bound state. There is, of course, the second pole but its behaviour does not influence an analytic structure of F near origin, so we shall not discuss it here. The orbit of the former one, which is of main interest for our discussion, is shown on Fig. 6.

The Omnés function has now the form

$$F(s;\, g) = \exp\left[\frac{s}{2\pi i}\int_4^{\infty}\frac{ds'}{s'(s'-s)}\log\frac{1-gA_3(s')/A_2(s')+g^2\varrho(s')A_2(s')\cdot i}{1-gA_3(s')/A_2(s')-g^2\varrho(s')A_2(s')\cdot i}\right] \tag{5.4}$$

and shapes of curves C_+ and C_- (Fig. 3) can be found more precisely. Functions A_2 and A_3 are given in Appendix C.

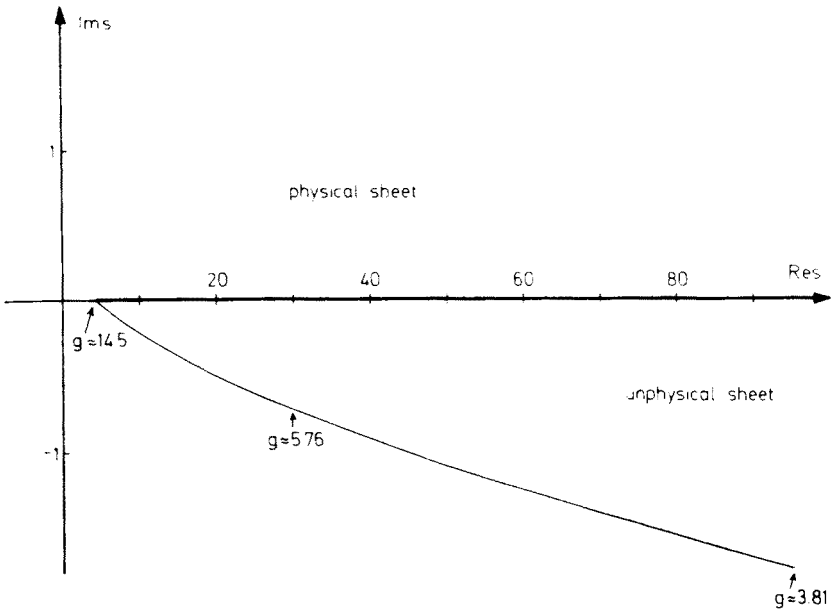

Fig. 6. The orbit of a pole of A in the simplified model

It can be shown that

$$A_2(s) \xrightarrow[s\to\infty]{} -\frac{5}{8\pi^2}+O(1/s); \qquad A_3(s) \xrightarrow[s\to\infty]{} \frac{5}{(2\pi)^4}\left(-\tfrac{11}{4}\log s\right)+O\left(\frac{\log s}{s}\right). \tag{5.5}$$

Therefore the singularities of the integrand as a function of g for $s' \to \infty$ can be found from

$$1-\alpha \log s' \cdot g \pm i\beta g^2 = 0, \tag{5.6}$$

where $\alpha, \beta > 0$. Now, we can easily see that

$$\operatorname{Re} g(s') \underset{s'\to\infty}{>} 0, \qquad \frac{\operatorname{Re} g(s')}{\operatorname{Im} g(s')} \xrightarrow[s'\to\infty]{} \infty \tag{5.7}$$

(for the root which goes to 0 for $s' \to \infty$) what means that $C_\pm$ are tangent to the positive axis at $g = 0$ (it can likewise be shown that they are tangent to real axis at $g = g_T$). The

other pole of A goes to ∞ both for $s' \to 4$ and $s' \to \infty$ what means that the only singularity of F other than $g = 0$ and $g = g_T$ is $g = \infty$. F can, therefore, be written as (after analytic continuation to the real axis — so it is rather F_e)

$$F_e(s; g) = \frac{1}{\pi} \int_0^{g_T} \frac{\Delta F(s; g')}{g' - g} dg' - \operatorname*{Re}_{g'=\infty} s \frac{F_e(s; g')}{g' - g}. \tag{5.8}$$

Using (3.7) and (3.8) we immediately see that

$$\begin{aligned} \Delta F(s; g') &= \frac{1}{2i}[F_e(s; g' + i\varepsilon) - F_e(s; g' - i\varepsilon)] \\ &= \frac{\operatorname{Im} s_{p+}(g')}{|s_{p+}(g')|^2} \cdot \frac{4s}{4 - s} F_O(s: g'), \end{aligned} \tag{5.9}$$

where $F_O(s; g')$ is the Omnés function for $g > 0$. $F_O(s; g') \to 1$ when $g' \to 0+$ because then $\delta^{T=1,\, l=1} \to 0$. Moreover, $s_{p+}(g) \sim \exp(-1/g)$ when $g \to 0$ what can be seen from (5.6). Thus

$$\int_0^{g_t} g'^{-n} \Delta F(s; g') dg'$$

exists for all n. As a result F_e is, for $s < 4$, a sum of a Stieltjes and of an entire function. Although it is well known that PA converge for both types of functions we do not know of any theorem that would apply to a sum. However, we find the following to be very plausible:

Hypothesis on Commutativity of Addition and Padeization (HCAP)

Let $[M/N]_f$, a sequence of PA to f, converge in capacity to f in some domain D_f, as $M, N \to \infty$ (somehow), and $[M/N]_g$, a sequence of PA to g, converge to g in capacity in some D_g when $M, N \to \infty$ in the same way; then $[M/N]_{f+g}$ converge in capacity to $f+g$ in $D_f \cap D_g$ for M, N as before.

It should be noted that even if $[M/N]$ converge to f and g uniformly, convergence of PA to $f+g$ can be, at most, in capacity. It is easily seen when f and g are both Stieltjes functions. Then the weight function for $f+g$ can, in general, change sign and poles of PA can then appear outside the support of the Stieltjes integral [11].

Assuming HCAP, we have for $s < 4$ convergence in capacity of $[N+k/N]_F$ to F_e in the whole complex plane except on the interval $(0, g_T)$ of the real axis. For $s \notin (0, 4)$, F is complex and we do not know anything about a convergence of PA for the first term in (5.8). We believe, however, that also in this case, paradiagonal sequences of PA converge in capacity in all the complex (g) plane except on $(0, g_T)$. Unfortunately, the only results on convergence of PA for functions with branch points — other than Stieltjes — concern PA built from Taylor series [12] and our belief can hardly be based on analogy with those results. However, independently of the detailed shape of a cut joining 0 and g_T, we expect that PA will reproduce F_e, which is not the physical formfactor. Moreover,

though F_e has poles on the real line (rather on the lower and upper lip of it, if the cut goes along the interval $(0, g_T)$), a convergence on it is, at most, slow (if the cut does not go along the real line, it is somewhere nearby and only asymptotically spurious poles of PA approach it at any finite order they are scattered in the neighbourhood and cause sharp oscillations there), or it does not appear at all.

Numerical calculations performed up to the eighth order fully support our expectations (coefficients of the perturbation expansion expressed by A_2 and A_3 are given in Appendix D; PA were calculated using an algorithm described in [13]). Although it was not possible

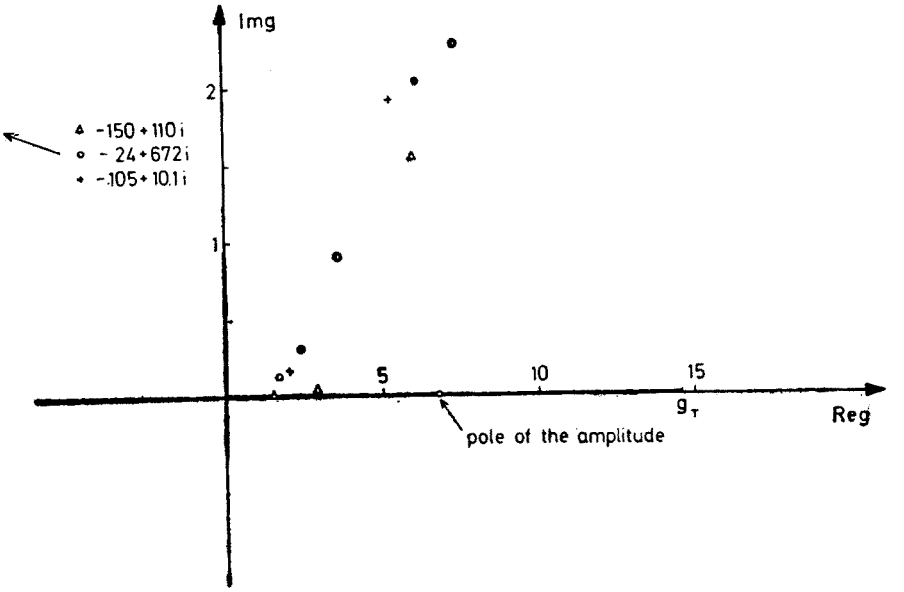

Fig. 7. Location of poles of diagonal and subdiagonal PA of F in the simplified model; poles of [2/3] ●, [3/3] +, [3/4] ○, [4/4] △, $s = 20-0.5i$ on the unphysical sheet

to determine a shape of the cut defined by PA, nevertheless the behaviour of their poles was in agreement with our considerations. For $s < 4$ poles of $[N+k/N]$ with $k \geqslant 1$ all lie in $(0, g_T)$, and for $k = 0, -1$ one of the poles is outside of this interval but still on the real line; none of these poles lie near the pole of the amplitude (we expect that for higher orders there would be more poles outside $(0, g_T)$ and that they would cluster at infinity for growing order — it can be proved that $g = \infty$ is an essential singularity in this model).

For $s \notin (0, 4)$ poles of $[N+k/N]$ lie near $(0, g_T)$ and for growing N approach it; $[N/N]$ and $[N-1/N]$ have, as before, one pole far in the complex plane. As before, none of these poles seem to approach the pole of the amplitude (Fig. 7). Orbits of all these poles form small loops around the threshold.

We have also tried to check an unusual behaviour of poles of $[0/N]$. It appeared that such a behaviour has been shown this time by poles of [0/4], [0/5], [0/6], [1/6], and [1/7] ([0/2] and [0/3] were identical as in Φ^4 because of obvious reasons). Though they behave

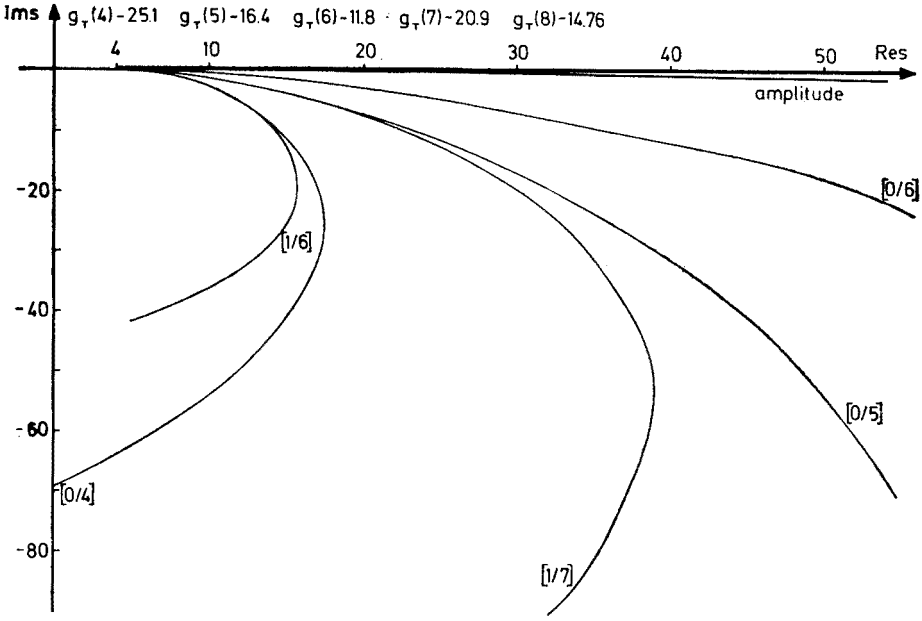

Fig. 8. Orbits of poles of [0/4], [0/5], [0/6], [1/6] and [1/7] in the simplified model

suspiciously, their orbits change quite irregularly when order of approximation increases, and their threshold values oscillate, so that we do not think they could approach the pole we are looking for (see Fig. 8).

6. *Conclusions*

We see that in the simplified model, considered in the last Section, it is probably impossible to reconstruct function F_i from the perturbation expansion of the Omnés function. Even if there is a slow convergence of PA on the interval $(0, g_T)$, they converge most probably to an analytically continued F_c. For $s < 4$ there is certainly (if we believe in HCAP) no convergence on this interval of g, and outside of it PA converge to F_c.

In the full Φ^4 model we were unable to reach definite conclusions on a location of cuts defined by PA. They depend on the features of the model unknown to us (a number of poles on the unphysical sheets and their detailed behaviour at $g \to 0$) and even if these were known, a lack of knowledge concerning a convergence of PA for functions with complicated singularities, would prevent us to correlate these features with domains of convergence of PA for F.

Nevertheless, we think that our arguments, supported then by numerical results obtained up to fourth order, show that low orders of perturbation expansion of F do not

contain sufficient information on the behaviour of F in the physical region ($g \in (0, g_T)$). It is even possible that it cannot be found from the perturbation expansion at all (if the right sector on Fig. 3 reduces to a straight line).

The only way out of this difficulty would be to insert somehow an additional information on a character of a singularity at $g = 0$, or to seek an expansion around another point.

The author would like to express his gratitude to Professor G. Białkowski for suggesting the study and for many valuable remarks and suggestions. Innumerable discussions with Dr L. Łukaszuk had the crucial importance for achieving results presented here. A discussion with Professor J. L. Basdevant has been also very important and his suggestion, pointed out in the text, helped, through the construction of the simplified model, to clarify many difficult questions.

APPENDIX A

$$
\begin{aligned}
F_2(s) = \frac{-5}{16(2\pi)^4}\Bigg\{ & -2\left[2+2\sqrt{\frac{s-4}{s}}\,L+\pi i\sqrt{\frac{s-4}{s}}\right] \\
& +8\left[-\frac{\pi^2}{24}-\frac{\pi^2}{3\sqrt{s(s-4)}}\,L+\frac{\pi i}{\sqrt{s(s-4)}}\,L^2\right. \\
& \left.+\frac{2}{3\sqrt{s(s-4)}}\,L^3\right]+8\left[\frac{\pi^2}{16}+\frac{\pi i}{s-4}\,L+\frac{1}{s-4}\,L^2\right] \\
& +16\left[\frac{2}{3(s-4)\sqrt{s(s-4)}}\,L^3+\frac{\pi i}{(s-4)\sqrt{s(s-4)}}\,L^2\right. \\
& \left.-\frac{\pi^2}{3(s-4)\sqrt{s(s-4)}}\,L-\frac{\pi^2}{12(s-4)}-\frac{\pi^2}{96}\right] \\
& +2\sqrt{\frac{s}{s-4}}\,L+\pi i\sqrt{\frac{s}{s-4}}\Bigg\},
\end{aligned}
\tag{A1}
$$

$$
\begin{aligned}
F_3(s) = \frac{-5}{8(2\pi)^6}\Bigg\{ & \tfrac{5}{8}\left[2+2\sqrt{\frac{s-4}{s}}\,L+\pi i\sqrt{\frac{s-4}{s}}\right] \\
& -\frac{117+8\pi^2}{6}\left[\frac{2}{\sqrt{s(s-4)}}\,L+\frac{\pi i}{\sqrt{s(s-4)}}-\tfrac{1}{2}\right] \\
& -\tfrac{3}{2}\left[L^2+\pi i L-\frac{\pi^2}{4}\right]-\frac{117+8\pi^2}{3}\left[\frac{1}{s-4}\,L^2\right. \\
& \left.+\frac{\pi i}{s-4}\,L+\frac{\pi^2}{16}\right]-\frac{4\pi^2}{3}\left[\frac{2}{3(s-4)}\sqrt{\frac{s}{s-4}}\,L^3\right.
\end{aligned}
$$

$$+\frac{\pi i}{s-4}\sqrt{\frac{s}{s-4}}\,L^2-\frac{\pi^2}{3(s-4)}\sqrt{\frac{s}{s-4}}\,L-\frac{\pi^2}{3(s-4)}-\frac{\pi^2}{12}\Bigg]$$

$$+34\left[\frac{2}{3(s-4)\sqrt{s(s-4)}}\,L^3+\frac{\pi i}{(s-4)\sqrt{s(s-4)}}\,L^2-\frac{\pi^2}{3(s-4)\sqrt{s(s-4)}}\,L\right.$$

$$\left.-\frac{\pi^2}{12(s-4)}-\frac{\pi^2}{96}\right]-7\left[\tfrac{2}{3}\frac{s}{s-4}\sqrt{\frac{s}{s-4}}\,L^3+\frac{s\cdot\pi i}{s-4}\sqrt{\frac{s}{s-4}}\,L^2\right.$$

$$\left.-\frac{s\cdot\pi^2}{s-4}\sqrt{\frac{s}{s-4}}\,L-\frac{4\pi^2}{3(s-4)}-\frac{\pi^2}{3}\right]-8\left[\frac{2}{3\sqrt{s(s-4)}}\,L^3+\frac{\pi i}{\sqrt{s(s-4)}}\,L^2\right.$$

$$\left.-\frac{\pi^2}{3\sqrt{s(s-4)}}\,L-\frac{\pi^2}{24}\right]-\tfrac{32}{3}\left[\frac{1}{2(s-4)}\,L^4+\frac{\pi i}{s-4}\,L^3\right.$$

$$\left.-\frac{\pi^2}{2(s-4)}\,L^2+\frac{\pi^4}{128}\right]-\tfrac{8}{3}\left[\frac{2}{5(s-4)}\sqrt{\frac{s}{s-4}}\,L^5\right.$$

$$+\frac{\pi i}{s-4}\sqrt{\frac{s}{s-4}}\,L^4-\frac{2\pi^2}{3(s-4)}\sqrt{\frac{s}{s-4}}\,L^3-\frac{\pi^4}{15(s-4)}\sqrt{\frac{s}{s-4}}\,L$$

$$\left.-\frac{\pi^4}{15(s-4)}-\frac{\pi^4}{60}\right]-\tfrac{7}{2}\left[\int_0^1\frac{(y+1)^2}{y(1-y)}\log^2 y\right.$$

$$\times\left(1+\frac{y+1}{y}\cdot\frac{1}{\sqrt[3]{s}\,\sqrt[3]{s-4}}\log\frac{1-y\sigma(s)}{1-y/\sigma(s)}\right)dy$$

$$\left.+\vartheta_{\text{nph}}\cdot\frac{\pi i}{\sqrt[3]{s}\,\sqrt[3]{s-4}}\int_1^{\sigma(s)}\frac{(y+1)^3}{y^2(1-y)}\log^2 y\,dy\right]-\frac{2\alpha}{(2\pi)^2}F_2(s)\Bigg\}. \tag{A2}$$

$$\alpha = 1+11/\sqrt{2}\arctan(1/\sqrt{2}), \tag{A3}$$

$$L = \log\frac{\sqrt{s}-\sqrt{s-4}}{2}, \tag{A4}$$

$$\sigma(s) = \left(\frac{\sqrt[3]{s}+\sqrt[3]{s-4}}{2}\right)^2, \tag{A5}$$

$$\vartheta_{\text{nph}} = \begin{cases} 0 & \text{on the physical sheet,} \\ 1 & \text{on the unphysical sheet.} \end{cases} \tag{A6}$$

$\sqrt[3]{x}$ means that the square root cut goes always from zero to infinity.

For other square roots a direction of the cut depends on what sheet we are. For physical sheet cuts go from zero to plus infinity, while on the unphysical one, they go from zero to minus infinity. This convention leaves values in the upper half plane unchanged and provides an analytic continuation to the lower half plane.

APPENDIX B

$$[0/2] = \frac{1}{1-g^2F_2}, \tag{B1}$$

$$[0/3] = \frac{1}{1-g^2F_2-g^3F_3}, \tag{B2}$$

$$[1/2] = \frac{1-gF_3/F_2}{1-gF_3/F_2-g^2F_2}, \tag{B3}$$

$$[2/1] = \frac{1-gF_3/F_2+g^2F_2}{1-gF_3/F_2}, \tag{B4}$$

$$[0/4] = \frac{1}{1-F_2g^2-F_3g^3+(F_2^2-F_4)g^4}, \tag{B5}$$

$$[1/3] = \frac{1+g(F_2^2-F_4)/F_3}{1+g(F_2^2-F_4)/F_3-g^2F_2-g^3[F_3+F_2(F_2^2-F_4)/F_3]}, \tag{B6}$$

$$[2/2] = \frac{1-gF_3/F_2+g^2[F_2+(F_3^2-F_4F_2)/F_2^2]}{1-gF_3/F_2+g^2(F_3^2-F_4F_2)/F_2^2}, \tag{B7}$$

$$[3/1] = \frac{1-gF_3/F_2+g^2F_2+g^3(F_3-F_2F_4/F_3)}{1-gF_4/F_3}. \tag{B8}$$

APPENDIX C

$$A_2^{T=1,I=1}(s) = A_2(s) = \frac{5}{8\pi^2}\left[-1+\frac{4}{s-4}+\frac{8}{s-4}\sqrt{\frac{s}{s-4}}\,L+\frac{8(s-2)}{(s-4)^2}\,L^2\right], \tag{C1}$$

$$A_3^{T=1,I=1}(s) = A_3(s) = \frac{5}{(2\pi)^4}\left\{\tfrac{5}{8}-\frac{117+8\pi^2}{6(s-4)}\right.$$

$$-\sqrt{\frac{s}{s-4}}\left[\tfrac{3}{2}+\frac{117+8\pi^2}{3(s-4)}\right]L$$

$$\left.-\left[\frac{4\pi^2s+21s^2-102}{3(s-4)^2}+\frac{8}{s-4}\right]L^2\right.$$

$$-\frac{32}{3(s-4)}\sqrt{\frac{s}{s-4}}\,L^3-\frac{8s}{3(s-4)^2}\,L^4+\frac{7}{4(s-4)}$$

$$\times\int_{\left(\frac{\sqrt{s}-\sqrt{s-4}}{2}\right)^2}^{1}\frac{(x+1)^3}{x^2(1-x)}\log^2 x\,dx\Bigg\}-\frac{\alpha}{2\pi^2}A_2(s). \tag{C2}$$

L and α mean the same as in Appendix A.

APPENDIX D

$$F(s;g)=1-g^2\frac{s}{\pi}I_0-g^3\frac{s}{\pi}I_1+g^4\left(-\frac{s}{\pi}I_2+\frac{s^2}{2\pi^2}I_0^2\right)$$

$$+g^5\left(-\frac{s}{\pi}I_3+\frac{s^2}{\pi^2}I_0I_1\right)+g^6\left(-\frac{s}{\pi}I_4+\frac{s^2}{\pi^2}I_0I_2\right.$$

$$\left.+\frac{s^2}{2\pi^2}I_1^2-\frac{s^3}{6\pi^3}I_0^3\right)+g^7\left(-\frac{s}{\pi}I_5+\frac{s^2}{\pi^2}I_0I_3\right.$$

$$\left.+\frac{s^2}{\pi^2}I_1I_2-\frac{s^3}{2\pi^3}I_0^2I_1\right)+g^8\left(-\frac{s}{\pi}I_6+\frac{s^2}{\pi^2}I_0I_4\right.$$

$$\left.+\frac{s^2}{\pi^2}I_1I_3+\frac{s^2}{2\pi^2}I_2^2-\frac{s^3}{2\pi^3}I_0^2I_2-\frac{s^3}{2\pi^3}I_0I_1^2+\frac{s^4}{24\pi^4}I_0^4\right), \tag{D1}$$

$$I_0(s)=\frac{1}{32\pi}\int_4^\infty\sqrt{\frac{s'-4}{s'}}\,\frac{A_2(s')}{s'(s'-s)}\,ds', \tag{D2}$$

$$I_1(s)=\frac{1}{32\pi}\int_4^\infty\sqrt{\frac{s'-4}{s'}}\,\frac{A_3(s')}{s'(s'-s)}\,ds', \tag{D3}$$

$$I_2(s)=\frac{1}{32\pi}\int_4^\infty\sqrt{\frac{s'-4}{s'}}\,\frac{A_3^2(s')}{A_2(s')}\,\frac{ds'}{s'(s'-s)}, \tag{D4}$$

$$I_3(s)=\frac{1}{32\pi}\int_4^\infty\sqrt{\frac{s'-4}{s'}}\,\frac{A_3^3(s')}{A_2^2(s')}\,\frac{ds'}{s'(s'-s)}, \tag{D5}$$

$$I_4(s) = \frac{1}{32\pi}\int_4^\infty \sqrt{\frac{s'-4}{s'}}\, A_2(s')\left[\frac{A_3^4(s')}{A_2^4(s')} - \tfrac{1}{3}\frac{s'-4}{s'}A_2^2(s')\right]\frac{ds'}{s'(s'-s)}, \tag{D6}$$

$$I_5(s) = \frac{1}{32\pi}\int_4^\infty \sqrt{\frac{s'-4}{s'}}\, A_3(s')\left[\frac{A_3^4(s')}{A_2^4(s')} - \frac{s'-4}{s'}A_2^2(s')\right]\frac{ds'}{s'(s'-s)}, \tag{D7}$$

$$I_6(s) = \frac{1}{32\pi}\int_4^\infty \sqrt{\frac{s'-4}{s'}}\,\frac{A_3^2(s')}{A_2(s')}\left[\frac{A_3^4(s')}{A_2^4(s')} - 2\frac{s'-4}{s'}A_2^2(s')\right]\frac{ds'}{s'(s'-s)}. \tag{D8}$$

REFERENCES

[1] G. A. Baker, Jr., *Essentials of Padé Approximants*, Academic Press 1975.

[2] J. Zinn-Justin, *Phys. Rep.* **C1**, 55 (1971); J. L. Basdevant, *Fortschr. Phys.* **20**, 283 (1972).

[3] C. R. Garibotti, M. Villani, *Nuovo Cimento* **61A**, 747 (1969); D. Masson, *Padé Approximants in Theoretical Physics*, Eds Baker and Gammel, Academic Press 1970, p. 231; D. Bessis, M. Villani, *J. Math. Phys.* **16**, 462 (1975); J. J. Loeffel et al., CERN preprint TH, 1103 (1969).

[4] D. Bessis, M. Pusterla, *Nuovo Cimento* **54A**, 243 (1968).

[5] L. A. Coppley, D. Masson, *Phys. Rev.* **164**, 2059 (1967).

[6] D. Bessis, M. Villani, see Ref. [3]; P. Mery, *Thése*, Université d'Aix–Marseille II (1976); D. Bessis, G. Turchetti, preprint CEN–Saclay DPh-T/76/131.

[7] J. Bjørken, D. Drell, *Relativistic Quantum Fields*, McGraw-Hill 1965.

[8] B. Bertolli et al., *Riv. Nuovo Cimento* **2**, 241 (1972).

[9] E. Ferrari, *Riv. Nuovo Cimento* **6**, 199 (1976).

[10] M. Pindor, *On Two Efficient Procedures ...*, preprint CPT, CNRS, Marseille 1976.

[11] D. Bessis, *Padé Approximants*, Ed. Graves Morris, The Institute of Physics 1973, p. 19.

[12] J. Nuttal, *The Convergence of Padé Approximants for a Class of Functions with Branch Points*, preprint, University of Western Ontario 1974; J. Nuttal, S. R. Singh, *J. Approx. Th.* **21**, 1 (1977).

[13] M. Pindor, *J. Comput. Appl. Math.* **1**, 141(1976).